Energetics of Nucleon and Photon Emission from Compound Nuclei: Angular Distributions of Cu^{61} Recoil Products*

MORTON KAPLAN† AND V. SUBRAHMANYAM
Department of Chemistry, Yale University, New Haven, Connecticut
(Received 1 August 1966)

We report the results obtained from a detailed study of the $Mn^{55}(B^{11},p4n)Cu^{61}$ reaction. The excitation function has a maximum cross section of about 130 mb at an energy corresponding to 6.2 MeV of available energy per nucleon emitted, and is in good agreement with the compound-nucleus reaction mechanism inferred earlier on the basis of recoil-range data. We have measured angular distributions of Cu^{61} at 10 bombarding energies over the region 53 to 114 MeV, covering all but the lowest-energy portion of the excitation function. These experiments have been analyzed to yield information on the average total energies of particles and photons emitted in the de-excitation of the compound nuclei. Above about 20 MeV of available energy, gamma-ray emission becomes significant and accounts for about 14 MeV of de-excitation energy at the higher bombarding energies. The amount of energy dissipated as gamma radiation is larger than nucleon binding energies, and indicates substantial competition between particle and photon emission in the de-excitation process. Our results are in very good agreement with the less specific but more direct gamma-ray measurements of other investigators.

I. INTRODUCTION

In a previous paper,[1] we reported measurements of average ranges and range distributions for Cu^{60} and Cu^{61} recoiling from several heavy-ion–induced nuclear reactions. The results obtained over a wide region of energy provided a sensitive test of the reaction mechanism, and led us to conclude that the observed Cu^{60} and Cu^{61} products were formed in compound-nucleus reactions. We have now directed our attention to one of these reactions, namely $Mn^{55}(B^{11},p4n)Cu^{61}$, and have carried out extensive studies in an attempt to derive information on the de-excitation properties of the highly excited compound nuclei.

We shall present below the results of excitation-function and angular-distribution experiments for Cu^{61} produced by bombardment of Mn^{55} with B^{11} ion beams. Angular-distribution data were obtained at ten bombarding energies over the region 53 to 114-MeV, covering all but the lowest energy portion of the excitation function. By means of the relationships to be described in the next section, we have analyzed the data in terms of a simple recoil-vector model and derived estimates of the average total energies of emitted nucleons and photons at each bombarding energy. The results obtained indicate that most of the de-excitation energy appears as kinetic energy of the emitted particles. However, the competition from gamma-ray emission is significant over much of the energy region investigated, accounting for approximately 14 MeV of de-excitation energy at the higher bombarding energies.

II. RELATIONSHIP OF REACTION DYNAMICS TO RECOIL ANGULAR DISTRIBUTIONS

The analysis of angular distributions of residual nuclei recoiling from compound nucleus reactions has been treated in detail by Simonoff and Alexander,[2] and has been presented previously.[2,3] Our derivation of the appropriate relationships is very similar to that of Ref. 2, but, by virtue of a slightly different approach, gives rise to equations which are somewhat less restrictive. We shall outline the development below, and indicate the differences from the earlier work.[2]

Consider a beam projectile of mass A_b and kinetic energy E_b reacting with a target nucleus of mass A_T to form a compound nucleus. The complete transfer of linear momentum from the incident beam results in a compound-nucleus velocity along the beam direction given by

$$v_c^2=2A_bE_b/(A_b+A_T)^2. \tag{1}$$

(v_c is also the velocity of the center of mass.) The emission of nucleons from the compound system imparts to the residual nucleus a resultant velocity V in the center-of-mass system, directed at a center-of-mass angle θ with respect to the incident beam. In the laboratory system, the recoil nucleus will appear at an angle θ_L given by

$$\tan\theta_L=\frac{V\sin\theta}{v_c+V\cos\theta}. \tag{2}$$

For all the recoiling nuclei, the laboratory angular distribution will have an average square tangent of the angle given by

$$\langle\tan^2\theta_L\rangle=\int_0^\pi\left[\frac{V\sin\theta}{v_c+V\cos\theta}\right]^2W(\theta)\sin\theta d\theta\Big/\times\int_0^\pi W(\theta)\sin\theta d\theta, \tag{3}$$

where $W(\theta)$ is the angular distribution of V. The

* Supported by the U. S. Atomic Energy Commission.
† Alfred P. Sloan Foundation Fellow.
[1] V. Subrahmanyam and M. Kaplan, Phys. Rev. **142**, 174 (1966).
[2] G. N. Simonoff and J. M. Alexander, Phys. Rev. **133**, B104 (1964).
[3] M. Kaplan and A. Ewart, Phys. Rev. **148**, 1123 (1966).

evaluation of Eq. (3) depends on the specific form of $W(\theta)$ and can be carried out explicitly in a number of cases. By rearranging the squared factor in the numerator and using the binomial series to expand $[1+(V/v_c)\cos\theta]^{-2}$, we have solved Eq. (3) for several commonly encountered forms of $W(\theta)$. This procedure requires only the condition that (V/v_c) be less than unity, in order to guarantee the convergence of the series expansion. We present below the resulting relationships, in each case assuming $(V/v_c)<1$.

Case 1, $W(\theta)=1$, isotropic emission:

$$\langle\tan^2\theta_L\rangle=\sum_{n=1}^{\infty}\frac{2\langle V^{2n}\rangle}{(2n+1)v_c^{2n}} \tag{4a}$$

$$=\frac{2\langle V^2\rangle}{3v_c^2}+\frac{2\langle V^4\rangle}{5v_c^4}+\frac{2\langle V^6\rangle}{7v_c^6}+\cdots. \tag{4b}$$

Case 2, $W(\theta)=a+b\cos^2\theta$, forward-backward peaking:

$$\langle\tan^2\theta_L\rangle=\sum_{n=1}^{\infty}\frac{2\langle V^{2n}\rangle[1+\{(2n-1)b/(2n+3)a\}]}{(2n+1)v_c^{2n}[1+(b/3a)]} \tag{5a}$$

$$=\frac{2\langle V^2\rangle[1+(b/5a)]}{3v_c^2[1+(b/3a)]}+\frac{2\langle V^4\rangle[1+(3b/7a)]}{5v_c^4[1+(b/3a)]}+\frac{2\langle V^6\rangle[1+(5b/9a)]}{7v_c^6[1+(b/3a)]}+\cdots. \tag{5b}$$

Case 3, $W(\theta)=1/\sin\theta$, extreme forward-backward peaking:

$$\langle\tan^2\theta_L\rangle=\sum_{n=1}^{\infty}\frac{(2n-1)!\langle V^{2n}\rangle}{(2^{2n-1})(n-1)!(n!)v_c^{2n}} \tag{6a}$$

$$=\frac{\langle V^2\rangle}{2v_c^2}+\frac{3\langle V^4\rangle}{8v_c^4}+\frac{15\langle V^6\rangle}{48v_c^6}+\cdots. \tag{6b}$$

In Eqs. (4)–(6), the quantities $\langle V^{2n}\rangle$ are the average $2n$th moments of the resultant velocities (in the center-of-mass system) imparted to the recoil nuclei by the emission of particles. Although Eq. (3) is written as if V were a unique quantity, there is in fact a distribution in the magnitudes of V, necessitating the introduction of the appropriate velocity averages.

The work of Simonoff and Alexander[2] analyzed the laboratory angular distributions in terms of the mean-square angle $\langle\theta_L^2\rangle$, rather than our choice of $\langle\tan^2\theta_L\rangle$. Their derivation then involved the expansion of an arc tangent function and neglect of terms of order higher than $(V/v_c)^2$ prior to performing the integration analogous to Eq. (3). This required the assumption $V\ll v_c$, and corresponded to the approximation $\langle\theta_L^2\rangle\approx\langle\tan^2\theta_L\rangle$. Their resulting equations for $\langle\theta_L^2\rangle$ yield first terms identical to those in Eqs. (4b), (5b), and 6(b), respectively, and hence when $V\ll v_c$ and $\langle\tan^2\theta_L\rangle\approx\langle\theta_L^2\rangle$ our equations reduce to theirs. The advantage of averaging over $\tan^2\theta_L$ lies in obtaining the complete equations (4a), (5a), and (6a) with no assumptions other than the convergence of series expansions (i.e., $V<v_c$). Since $\langle\tan^2\theta_L\rangle$ is an experimentally determined quantity, one can then decide in any given situation which approximations are appropriate.[4] It should be noted that $\langle\tan^2\theta_L\rangle$ is always greater than $\langle\theta_L^2\rangle$.

Equations (4)–(6) relate a characteristic of the laboratory angular distribution to the magnitudes of the center-of-mass velocity v_c and the recoil velocity in the center-of-mass system, V. The former quantity is given by Eq. (1) for compound nucleus reactions, and is considered a known quantity in our experiments. On the other hand, the average moments of V are complex quantities, related to the detailed energy and angular distributions of the evaporated particles, and are not generally describable in simple form. However, in the special but common case of isotropic nucleon emission by the compound nucleus, it has been shown[2] that

$$\langle V^2\rangle=\frac{8T_n}{(A_T+A_b+A_R)^2}, \tag{7}$$

where T_n is the average total kinetic energy of the emitted nucleons in the center-of-mass system and A_R is the mass of the residual nucleus. If one now imposes the condition $V\ll v_c$ and retains only the leading term in Eq. (4), then combination of Eqs. (1), (4), and (7) yields for $W(\theta)=1$, the relation

$$T_n=\frac{3E_bA_b(A_b+A_T+A_R)^2}{8(A_b+A_T)^2}\langle\tan^2\theta_L\rangle. \tag{8}$$

When nucleon emission is not isotropic, but is enhanced in the forward-backward direction, then an observed $\langle\tan^2\theta_L\rangle$ would correspond to a somewhat larger value of T_n then indicated by Eq. (8). Although such anisotropic situations imply a correlation between emission velocity and center-of-mass emission angle, one may ignore any such dependence of V on θ and thereby obtain[5] for $W(\theta)=a+b\cos^2\theta$ and $V\ll v_c$,

$$T_n=\frac{3E_bA_b(A_b+A_T+A_R)^2[1+(b/3a)]}{8(A_b+A_T)^2[1+(b/5a)]}\langle\tan^2\theta_L\rangle. \tag{9}$$

Similarly, for $W(\theta)=1/\sin\theta$ and $V\ll v_c$,

$$T_n=\frac{E_bA_b(A_T+A_b+A_R)^2}{2(A_b+A_T)^2}\langle\tan^2\theta_L\rangle. \tag{10}$$

[4] The experiments reported in Ref. 2 yielded average angles sufficiently small for the distinction between $\langle\tan^2\theta_L\rangle$ and $\langle\theta_L^2\rangle$ to be neglected. In the present work, however, the average angles are larger, and the difference between $\langle\tan^2\theta_L\rangle$ and $\langle\theta_L^2\rangle$ is approximately 3%.

[5] J. M. Alexander, J. Gilat, and D. H. Sisson, Phys. Rev. **136**, B1289 (1964).

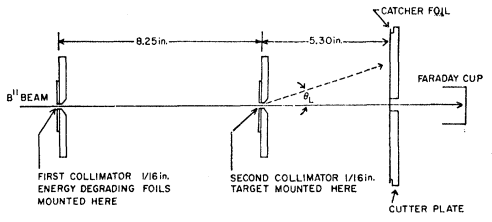

FIG. 1. Schematic diagram of the apparatus used in angular-distribution experiments.

These equations correspond to the ones presented by Alexander, Gilat, and Sisson,[5] with $\langle\theta_L^2\rangle$ replaced by $\langle\tan^2\theta_L\rangle$.

The average total energy involved in electromagnetic de-excitation processes may be obtained by subtracting T_n from the total energy available:

$$T_\gamma=(E_{\text{c.m.}}+Q)-T_n. \tag{11}$$

As can be seen from Eqs. (8)–(10), the values of average total kinetic energy of emitted nucleons derived from measurements of $\langle\tan^2\theta_L\rangle$ are not very sensitive to the assumed form of $W(\theta)$. The effect on the T_n values resulting from neglect of higher terms in Eqs. (4)–(6) may be estimated by successive approximations, and corrections applied where necessary. It is the general utility of these relationships that provides the basis for the experiments we shall describe below.

III. EXPERIMENTAL PROCEDURES

Two types of experiment were performed in the present work, cross-section measurements and angular-distribution studies. The cross-section experiments utilized a stacked-foil technique in which several Mn^{55} targets, Al recoil-catcher foils, and blank foils were assembled in a water-cooled holder and irradiated with a beam of B^{11} ions from the Yale heavy-ion linear accelerator. The targets consisted of thin layers of Mn metal (99.5% purity) evaporated onto 0.00025-in. Al backings. The recoil catchers and blank foils were 1-in. disks of 0.0005- or 0.00025-in. Al. Target and Al foil thicknesses were individually determined by weight and area measurements. The HILAC beam was defined by two $\frac{1}{4}$-in. collimators 20 in. apart located 10 in. from the target holder. In some experiments, the full beam energy of 115.5 MeV was incident on the target stack, while in other experiments lower incident energies were obtained by inserting appropriate Al foils in the beam path and magnetically analyzing the degraded beam upstream from the collimator assembly. Beam energies in the targets were calculated from the energy-loss data of Northcliffe.[6] Integrated beam fluxes were obtained with a magnetically shielded Faraday cup and Elcor electrometer.

Following bombardment, the foil stack was separated and copper isolated by radiochemical analysis. The foils were dissolved in HCl, Cu^{++} and Fe^{3+} carriers were added, and $Fe(OH)_3$ was precipitated by an excess of ammonium hydroxide. Copper remained in solution as an ammonia complex, and was separated from the scavenging precipitate by centrifugation. Samples were prepared for counting by reduction to metallic copper with ammonium hypophosphite, or by precipitation as cuprous thiocyanate following reduction with potassium sulfite.

The purified samples were assayed for β radioactivity on a series of end-window methane-flow proportional counters. The counters were intercalibrated with a thick uranium source and their discriminator levels adjusted to yield equal counting efficiencies within 1%. Intercalibration with Cu^{61} sources showed no difference in relative counter efficiencies. The samples were counted periodically for at least 7 h to verify the radiochemical purity of 3.3-h Cu^{61}. The counting data were corrected for counter background, chemical yield of the sample (obtained by iodimetric determination of copper after counting), and activation of the catcher foils. The foil activation was determined from the activity induced in blank foils.

In a separate series of experiments, the absolute detection efficiencies of the β counters for Cu^{61} were determined by counting samples whose disintegration rates were known. The disintegration rates were computed from γ-γ coincidence and γ-singles intensity measurements.

The angular distribution experiments were performed in the apparatus described previously.[3] A schematic diagram is shown in Fig. 1. Recoil nuclei escaping from a thin target traveled in vacuum and were caught on a catcher plate located at a known distance from the target. The catcher plate consisted of a 4-in.-diam stainless-steel cutter, with sharp circular blades accurately machined at $\frac{1}{8}$-in. radial intervals. Aluminum foil, 0.001 in. thick, was stretched over the cutting edges and after collection of recoils, the foil was cut into rings by means of an hydraulic press. Each ring corresponded to a well-defined angular interval whose value was determined by the calibration procedure described previously.[3] In the present experiments, the target-catcher distance was chosen to yield an angular acceptance of approximately 1.3° per ring.

The residual nuclei recoiling from compound nucleus reactions induced by heavy ions are kinematically restricted to relatively small forward angles. Physically, this is a consequence of the momentum transfer in the initial collision being much larger than the resultant from subsequent nucleon evaporation. In order to obtain adequate angular resolution in our experiments, it was therefore necessary for the incident projectile beam to be highly collimated. Most of our experiments employed two $\frac{1}{16}$-in.-diam graphite collimators (see Fig. 1), but in several runs one or both of these were enlarged to $\frac{1}{8}$-in. diameter. The increase in collimator

[6] L. C. Northcliffe, Phys. Rev. **120**, 1744 (1960); Ann. Rev. Nucl. Sci. **13**, 67 (1963).

size did not produce any significant change in the observed angular distributions.

After bombardment, the catcher foil was cut, each ring chemically processed, and the samples assayed for Cu^{61} as described above. As only relative activity measurements are required for each angular distribution, absolute counter efficiency corrections were not applied to the data.

The effects of target thickness on the angular distributions have been investigated in some detail by measuring the target-thickness dependence at five bombarding energies spanning the region of our experiments. This will be discussed more fully in Sec. IV below.

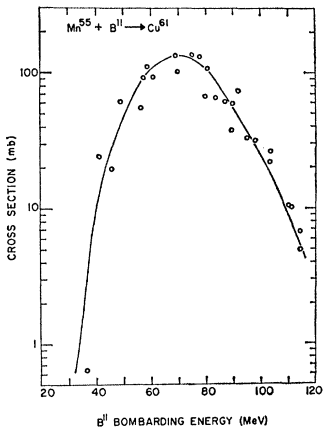

FIG. 2. Excitation function for the Mn^{55}-$(B^{11},p4n)Cu^{61}$ reaction

IV. RESULTS AND DISCUSSION

In this paper we report a study of the $Mn^{55}(B^{11},p4n)$-Cu^{61} reaction, although our measurements would not distinguish this process from the competing Mn^{55}-$(B^{11},5n)Zn^{61}$ reaction (followed by β decay to Cu^{61}). Investigations of competitive decay channels for compound nuclei in this mass region have indicated that reactions in which a proton is emitted are considerably more probable than corresponding pure neutron-emission reactions.[7] In our work, the threshold energy for direct Cu^{61} production is 31.9 MeV ($Q=-26.6$ MeV) while the Zn^{61} reaction requires 39.9 MeV ($Q=-33.2$ MeV). Therefore, it is likely that the primary source of Cu^{61} is the $(B^{11},p4n)$ reaction, but it is possible that the $(B^{11},5n)$ process contributes significantly to the data. However, for our purposes, it is not vital that such a distinction be made between the alternate reaction paths, as the conclusions we shall reach are not appreciably different for the two cases.

We present our cross-section data in Table I and the corresponding excitation function in Fig. 2. On the basis of recoil-range evidence reported earlier,[1] we concluded that the $Mn^{55}(B^{11},p4n)Cu^{61}$ reaction proceeded by a compound-nucleus mechanism, and the character of the excitation function in Fig. 2 is consistent with this interpretation (i.e., the cross section increases rapidly above threshold, passes through a maximum, and then decreases with increasing bombarding energy). The peak cross section occurs at an energy corresponding to 6.2 MeV of available energy ($E_{c.m.}+Q$) per emitted nucleon, which is similar to the results obtained for Dy[8] and Sm[9] products from a large number of heavy-ion–induced compound nucleus reactions.

TABLE I. Cross-section results for the $Mn^{55}(B^{11},p4n)Cu^{61}$ reaction.

Bombarding energy, E_b (MeV)	Cross section, σ (mb)	Bombarding energy, E_b (MeV)	Cross section, σ (mb)
114.0	4.9	79.5	67.2
113.9	6.7	77.4	130.5
110.0	10.2	74.6	136.8
109.5	10.4	69.3	101.4
102.8	26.0	68.6	133.2
102.7	22.1	60.4	93.0
97.5	31.4	58.5	112.2
94.6	32.9	57.1	91.2
91.7	73.1	56.2	55.2
89.5	58.5	49.4	61.2
89.1	37.4	45.7	19.5
86.5	61.2	41.3	24.3
83.6	65.1	36.1	0.6
80.5	106.8		

Angular-distribution experiments were carried out at ten bombarding energies from 53 to 114 MeV. The cylindrical geometry of our apparatus was such that the radioactivity in a catcher ring is proportional to $d\sigma/d\theta_L$, corresponding to the angular interval subtended by the ring. We have analyzed our data in the following manner. For each ring, we have evaluated (σ_i/σ), where σ_i is proportional to the cross section in the angular interval of ring i, and σ is the total cross section. The ratio (σ_i/σ) is equivalent to the fractional activity found in ring i. The quantity $\langle\tan^2\theta_L\rangle$ for the angular distribution was then obtained from :

$$\langle\tan^2\theta_L\rangle=\textstyle\sum_i(\sigma_i/\sigma)\langle\tan^2\theta_i\rangle. \tag{12}$$

The factor $\langle\tan^2\theta_i\rangle$ is the average square tangent of the angle subtended by ring i, and is given by

$$\langle\tan^2\theta_i\rangle=\sec\theta_2\sec\theta_1-1, \tag{13}$$

where θ_2 and θ_1 are the defining angles of the ring.[10] We have also computed the average angle $\langle\theta_L\rangle$ and the mean square angle $\langle\theta_L^2\rangle$ for each experiment, using similar equations.

[7] J. P. Hazan and M. Blann, Phys. Rev. **137**, B1202 (1965); C. F. Smith, Jr., University of California Radiation Laboratory Report No. UCRL-11862, 1965 (unpublished).

[8] J. M. Alexander and G. N. Simonoff, Phys. Rev. **133**, B93 (1964).

[9] M. Kaplan, Phys. Rev. **143**, 894 (1966).

[10] Equation (13) is obtained by evaluating:

$$\langle\tan^2\theta_i\rangle=\int_{\theta_1}^{\theta_2}\tan^2\theta\sin\theta d\theta\Big/\int_{\theta_1}^{\theta_2}\sin\theta d\theta.$$

TABLE II. Angular distribution results for the $Mn^{55}(B^{11},p4n)Cu^{61}$ reaction.

Bombarding energy, E_b (MeV)	Target thickness, W ($\mu g/cm^2$)	Angular interval (deg) / Ring No.	0.00 1	1.35 2	2.71 3	4.06 4	5.40 5	6.74 6	8.07 7	9.39 8	10.71 9	12.00 10	13.30 11	14.58 12	15.84 13	17.10 14	18.30 15	19.54 16	20.70	$\langle\theta_L\rangle$ (deg)	$100\langle\theta_L^2\rangle$ (rad^2)	$100\langle\tan^2\theta_L\rangle$
			Fractional cross section, σ_i/σ																			
53.3	427		0.054	0.069	0.088	0.104	0.111	0.104	0.096	0.081	0.066	0.054	0.046	0.036	0.030	0.023	0.019	0.015		8.29	2.81	2.95
53.3[a]	320		0.039	0.058	0.083	0.107	0.119	0.113	0.107	0.087	0.071	0.056	0.044	0.034	0.025	0.019	0.015	0.011		8.15	2.69	2.80
53.3[a]	95		0.044	0.060	0.082	0.111	0.128	0.123	0.106	0.084	0.067	0.050	0.038	0.030	0.024	0.019	0.014	0.012		7.92	2.59	2.71
57.9[b]	405		0.043	0.061	0.086	0.106	0.116	0.117	0.117	0.088	0.066	0.053	0.041	0.032	0.025	0.019	0.015	0.012		8.20	2.68	2.80
57.9[b]	215		0.058	0.075	0.096	0.113	0.123	0.120	0.104	0.083	0.065	0.049	0.036	0.027	0.019	0.014	0.011	0.008		7.63	2.35	2.45
57.9[b]	97		0.072	0.085	0.099	0.116	0.123	0.114	0.094	0.076	0.058	0.044	0.036	0.027	0.020	0.015	0.011	0.009		7.39	2.29	2.39
64.5	427		0.042	0.058	0.077	0.100	0.119	0.126	0.111	0.093	0.077	0.060	0.045	0.032	0.024	0.017	0.012	0.008		8.26	2.66	2.78
69.9	427		0.046	0.062	0.086	0.106	0.115	0.115	0.109	0.096	0.078	0.062	0.045	0.029	0.020	0.013	0.009	0.007		8.05	2.55	2.65
69.9	95		0.028	0.052	0.092	0.135	0.153	0.147	0.123	0.092	0.065	0.040	0.026	0.019	0.013	0.008	0.006	0.004		7.49	2.13	2.22
69.9	47		0.042	0.056	0.084	0.112	0.133	0.147	0.140	0.110	0.073	0.046	0.024	0.015	0.008	0.004	0.003	0.001		7.45	2.10	2.17
74.3[c]	427		0.027	0.040	0.061	0.085	0.110	0.121	0.113	0.102	0.085	0.071	0.056	0.044	0.032	0.023	0.017	0.013		9.11	3.14	3.28
77.3[b]	405		0.043	0.063	0.088	0.107	0.120	0.122	0.112	0.089	0.071	0.054	0.041	0.030	0.022	0.016	0.012	0.008		8.08	2.57	2.68
84.2	427		0.039	0.053	0.071	0.092	0.111	0.120	0.114	0.099	0.083	0.063	0.050	0.038	0.026	0.019	0.014	0.010		8.60	2.86	2.99
96.8	427		0.055	0.067	0.084	0.101	0.110	0.110	0.101	0.089	0.072	0.055	0.044	0.035	0.027	0.021	0.017	0.014		8.24	2.75	2.88
104.3[b]	405		0.041	0.054	0.072	0.095	0.110	0.112	0.107	0.096	0.081	0.066	0.051	0.038	0.028	0.021	0.016	0.011		8.66	2.91	3.04
104.3[b]	215		0.043	0.060	0.080	0.097	0.107	0.122	0.109	0.098	0.080	0.063	0.049	0.037	0.026	0.018	0.012	0.008		8.37	2.75	2.87
104.3[b]	95		0.041	0.055	0.072	0.088	0.105	0.117	0.114	0.099	0.083	0.063	0.048	0.037	0.027	0.021	0.015	0.012		8.66	2.91	3.04
114.0	427		0.039	0.051	0.068	0.087	0.102	0.105	0.102	0.094	0.082	0.068	0.057	0.048	0.036	0.027	0.020	0.015		9.06	3.19	3.33
114.0	97		0.046	0.057	0.062	0.081	0.095	0.110	0.116	0.107	0.087	0.064	0.049	0.039	0.031	0.024	0.018	0.015		8.77	3.04	3.18
114.0	47		0.031	0.045	0.063	0.085	0.106	0.113	0.113	0.100	0.085	0.070	0.053	0.041	0.031	0.023	0.017	0.013		8.89	3.06	3.19

[a] Second collimator $\frac{1}{8}$-in. diam. [b] Both collimators $\frac{1}{8}$-in. diam. [c] This experiment was carried out with a B^{10} beam.

$$\langle\theta_L\rangle=\sum_i(\sigma_i/\sigma)\langle\theta_i\rangle;\quad \langle\theta_i\rangle=(\theta_1+\theta_2)/2. \tag{14}$$

$$\langle\theta_L^2\rangle=\sum_i(\sigma_i/\sigma)\langle\theta_i^2\rangle;\quad \langle\theta_i^2\rangle=(\theta_1^2+\theta_1\theta_2+\theta_2^2)/3. \tag{15}$$

The average laboratory angle $\langle\theta_L\rangle$ is useful because it gives some physical feeling for the distribution. The mean square angle $\langle\theta_L^2\rangle$ has been tabulated to illustrate the magnitude of its deviation from $\langle\tan^2\theta_L\rangle$.

Our angular distribution data are given in Table II. Each experiment corresponds to a horizontal row across the table. The first two columns list, respectively, the bombarding energy and target thickness in the experiment. Then we show the fractional cross section, (σ_i/σ), measured for each ring. Also indicated is the angular acceptance of each ring. Finally, the last three columns contain the average quantities $\langle\theta_L\rangle$, $\langle\theta_L^2\rangle$, and $\langle\tan^2\theta_L\rangle$ for each angular distribution.

Figure 3 is a typical set of angular distributions for Cu^{61}, obtained at one energy with targets of different thickness. The parimary effect of target thickness is to broaden the angular distribution, presumably by scattering of the recoils into larger angles. As the computed averages $\langle\tan^2\theta_L\rangle$ are quite sensitive to the cross section at large angles, we have measured the target-thickness dependence at five different energies and extrapolated the results to zero target thickness. These investigations are summarized in Fig. 4.

As can be seen from Fig. 4, the change in $\langle\tan^2\theta_L\rangle$ with target thickness is energy-dependent. At 114.0-MeV bombarding energy, the empirical slope is 4.22×10^{-6} $(\mu g/cm^2)^{-1}$, whereas at 69.9 MeV the slope is 12.9×10^{-6} $(\mu g/cm^2)^{-1}$. The resulting corrections to zero target thickness are thus substantial (varying between 5% and 20% for the thickest targets), but not very sensitive to uncertainties in the slopes. At bombarding energies where target thickness studies were not carried out experimentally, the angular distributions were corrected by interpolating the appropriate slopes from the data in Fig. 4.

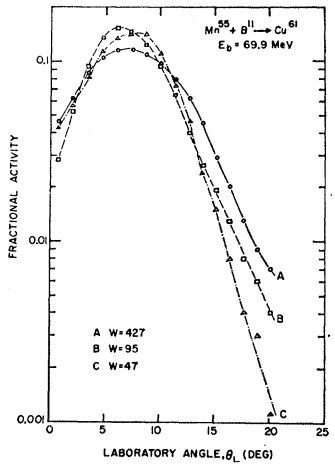

FIG. 3. Typical appearance of Cu^{61} angular distributions from the $Mn^{55}(B^{11},p4n)$ reaction. The three curves are for different target thicknesses as indicated ($\mu g/cm^2$).

An interesting feature of our results is that $\langle\tan^2\theta_L\rangle$ does not vary monotonically with bombarding energy, but passes through a minimum in the vicinity of 70 MeV.[11] (This can be seen from Table II or Fig. 4.) Reference to Eqs. (4)–(6) indicates that $\langle\tan^2\theta_L\rangle$ depends primarily on the ratio $\langle V^2\rangle/v_c^2$, and from Eq. (1) we know that v_c^2 increases linearly with bombarding energy. Hence the observed energy dependence of $\langle\tan^2\theta_L\rangle$ reflects a nonlinear variation of $\langle V^2\rangle$ with energy. At our lower energies, $\langle V^2\rangle$ is increasing less rapidly than v_c^2 and at the higher energies $\langle V^2\rangle$ increases more rapidly than v_c^2. We shall attempt to show below that this behavior arises from the effects of gamma-ray emission in the de-excitation of the compound nuclei.

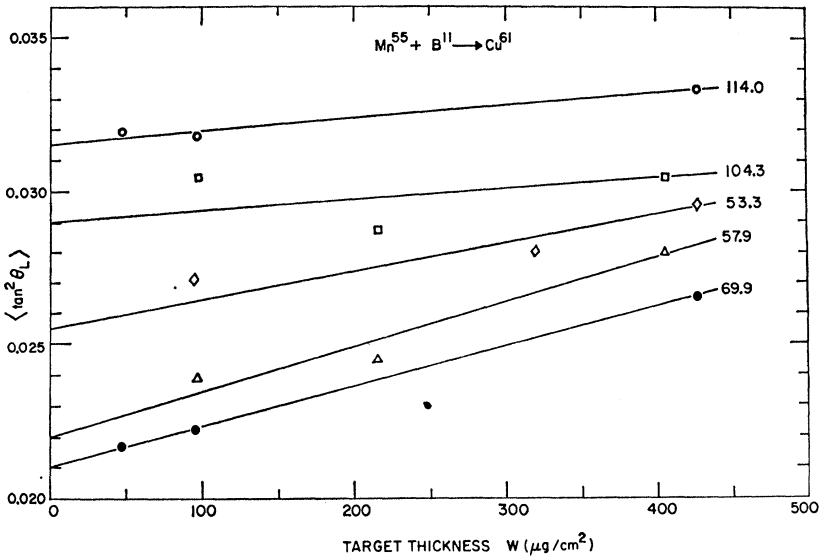

FIG. 4. Experimental dependence of the quantity $\langle\tan^2\theta_L\rangle$ on target thickness, for Cu^{61} recoiling from the $Mn^{55}(B^{11},p4n)$ reaction. The numbers to the right of each line designate the bombarding energy in MeV.

[11] By what must surely be coincidence, the minimum in $\langle\tan^2\theta_L\rangle$ happens to occur at the maximum in the excitation function.

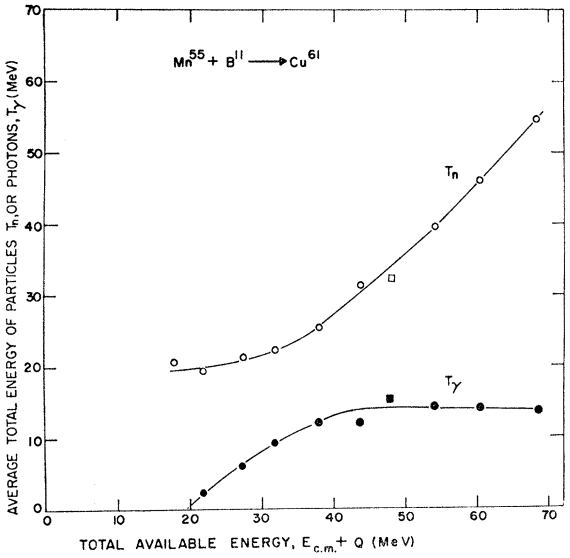

FIG. 5. Average total energies of particles T_n, and photons T_γ, plotted against total available energy in the c.m. system, for the $Mn^{55}(B^{11},p4n)Cu^{61}$ reaction. (The square points at $E_{c.m.}+Q=47.8$ MeV are from a B^{10} experiment.)

In order to relate our experimental quantities to the energetics of the de-excitation process, by means of the analysis in Sec. II, we must make an assumption concerning the form of $W(\theta)$ .Since $W(\theta)$ is the center-of-mass angular distribution of V, and each V is the resultant of several successive nucleon emissions, it is reasonable to assume $W(\theta)=1$. Even if there is some anisotropic character in an individual nucleon emission, the effect on V will be considerably diluted. In the remainder of this paper, we shall assume isotropy of V. [Comparisons of experimental recoil angular distributions with theoretical calculations[12] have indicated that the assumption $W(\theta)=1$ is indistinguishable, within experimental uncertainty, from $W(\theta)=a+b\times\cos^2\theta$ for $(b/a)<\sim 1$.]

TABLE III. Average recoil angles and derived average total energies of particles and photons for the $Mn^{55}(B^{11},p4n)Cu^{61}$ reaction.

Bombarding energy, E_b (MeV)	$\langle\tan^2\theta_L\rangle$[a]	Total available energy ($E_{c.m.}+Q$) (MeV)	Average total particle energy, T_n(MeV)	Average total photon energy, T_γ(MeV)
53.3	2.55×10^{-2}	17.8	20.7	−2.9
57.9	2.20	21.7	19.4	2.3
64.5	2.17	27.1	21.4	5.7
69.9	2.10	31.7	22.4	9.3
77.3	2.17	37.8	25.6	12.2
84.2	2.44	43.5	31.4	12.1
74.3[b]	3.09	47.8	32.4	15.4
96.8	2.69	54.0	39.7	14.3
104.3	2.90	60.3	46.2	14.1
114.0	3.15	68.4	54.8	13.6

[a] Corrected to zero target thickness.
[b] This experiment was with a B^{10} beam.

[12] A. Ewart and M. Kaplan (unpublished).

Table III presents our corrected angular distribution results and the de-excitation energies derived from them. The first two columns list, respectively, the bombarding energy and the value of $\langle\tan^2\theta_L\rangle$ at zero target thickness. Column 3 is the total energy available in the center-of-mass system, given by $E_{c.m.}+Q$. This energy is distributed into the c.m. kinetic energies of particle emission and into gamma-ray production. The fourth column contains the average total kinetic energy of the emitted nucleons, T_n, obtained from the data in column 2 by means of Eq. (8). The last column is the average total energy dissipated as photons, T_γ, which is given by Eq. (11) as the difference between columns 3 and 4.

Exclusive of systematic errors, we estimate the uncertainty in the T_n values to be about 1 MeV over most of the energy range, and somewhat larger at the lowest bombarding energies. This uncertainty arises directly [see Eq. (8)] from the measurements of $\langle\tan^2\theta_L\rangle$ and E_b. Random errors of similar magnitude are introduced into the T_γ results. Systematic experimental errors, if present, would generally tend to broaden the angular distributions,[3] leading to an overestimation of T_n and underestimation of T_γ. Hence, in one sense the values in Table III may be considered as upper and lower limits for T_n and T_γ, respectively, but it is unlikely that they differ very much from the true values.

We show in Fig. 5 the values of T_n and T_γ plotted as a function of $E_{c.m.}+Q$. At about 20 MeV of available energy, gamma-ray emission begins to be a significant source of energy release, rising to about 14 MeV and then remaining approximately constant with increasing available energy. The kinetic energies of emitted particles, meanwhile, do not change very much over the region where gamma-ray energy is increasing. When the gamma-ray energy has leveled off, additional energy put into the system results in the rapid increase of particle kinetic energies. We would infer from Fig. 5 that below about 20-MeV available energy, there is no appreciable gamma-ray production (less than about 2 MeV) and the T_n curve should be approximately equal to $E_{c.m.}+Q$ down to zero energy. It is unfortunate that a rapidly decreasing reaction cross section prevents our obtaining measurements in this region.

Of particular significance is our finding that, in the $Mn^{55}(B^{11},p4n)Cu^{61}$ reaction, the total gamma-ray energy rises to values considerably larger than nucleon binding energies. This result would imply a substantial competition between photon and particle emission, and is very likely a consequence of high angular-momentum deposition in the compound nuclei.[13]

The variation of total gamma-ray energy with available energy in Fig. 5 is different from the behavior reported for some other compound-nucleus reactions. Simonoff and Alexander,[2] in studying angular distributions of Dy recoil products, found a consistent increase of T_γ with energy at comparable excitation energies.

[13] J. R. Grover, Phys. Rev. **127**, 2142 (1962).

On the other hand, Kaplan and Ewart[3] observed relatively little gamma-ray emission from Cl^{34} over an energy range extending to even higher excitation energies. Hence, it would appear that the characteristics of gamma-ray competition with particle emission are strongly related to the mass region being considered, presumably through differences in level densities and availability of angular momentum states at high excitation.[14]

It is worthwhile to compare our T_γ results with direct measurements of gamma-ray energies. Mollenauer[15] has compared the gamma-ray yields for compound nucleus reactions induced by C^{12} and He^4 ions in several targets, and has observed enhanced photon production in the heavy-ion bombardments. Our value of $T_\gamma=14$ MeV for Cu^{61} is in excellent agreement with his result of 12 MeV for the total gamma-ray energy released in $C^{12}+V^{51}$ reactions (to give Cu compound nuclei) at very similar excitation energies. The work of Oganesyan *et al.*[16] on gamma rays from $Cu+Ne^{22}$ has concluded that about 9 MeV is released at somewhat lower excitation energies .Although our $Mn^{55}+B^{11}$ reaction is appreciably removed from this process, we would predict from Fig. 5 that $T_\gamma=10$ MeV at these lower energies.

In summary, our studies of the $Mn^{55}(B^{11},p4n)Cu^{61}$ reaction have led to the following conclusions. (a) The excitation function behavior is consistent with the compound-nucleus reaction mechanism inferred earlier on the basis of recoil-range data. (b) At low energies, essentially all of the available energy is removed as kinetic energies of emitted particles. Above about 20 MeV of available energy, gamma-ray emission becomes significant, rising to about 14 MeV and then remaining constant with increasing energy. (c) The amount of energy dissipated as gamma radiation is larger than nucleon binding energies, and indicates competition between particle and photon emission in the deexcitation process. (d) Our indirect determination of the total gamma-ray energy release is in very good agreement with the less specific, but more direct, measurements of other investigators.

ACKNOWLEDGMENTS

We extend our appreciation to the operating staff of the Yale HILAC for their extra efforts in getting beam through our collimators, and to Professor John M. Alexander for many helpful discussions.

[14] J. R. Grover and J. Gilat, Brookhaven National Laboratory Report No. BNL 10427 (unpublished), J. R. Grover, Brookhaven National Laboratory Report BNL 10428 (unpublished).
[15] J. F. Mollenauer, Phys. Rev. **127**, 867 (1962).
[16] Y. T. Oganesyan, Y. V. Lobanov, B. N. Markov, and G. N. Flerov, Zh. Eksperim. i Teor. Fiz. **44**, 1171 (1963) [English transl.: Soviet Phys.—JETP **17**, 791 (1963)].